Predicting errors from reconfiguration patterns in human brain networks

Matthias Ekman[a,b,1], Jan Derrfuss[a,b], Marc Tittgemeyer[b], and Christian J. Fiebach[a,c,d]

[a]Radboud University Nijmegen, Donders Institute for Brain, Cognition, and Behaviour, Nijmegen 6500 HE, The Netherlands; [b]Max Planck Institute for Neurological Research, 50931 Cologne, Germany; [c]Department of Psychology, Goethe University Frankfurt, 60325 Frankfurt am Main, Germany; and [d]Center for Individual Development and Adaptive Education, 60486 Frankfurt am Main, Germany

Task preparation is a complex cognitive process that implements anticipatory adjustments to facilitate future task performance. Little is known about quantitative network parameters governing this process in humans. Using functional magnetic resonance imaging (fMRI) and functional connectivity measurements, we show that the large-scale topology of the brain network involved in task preparation shows a pattern of dynamic reconfigurations that guides optimal behavior. This network could be decomposed into two distinct topological structures, an error-resilient core acting as a major hub that integrates most of the network's communication and a predominantly sensory periphery showing more flexible network adaptations. During task preparation, core–periphery interactions were dynamically adjusted. Task-relevant visual areas showed a higher topological proximity to the network core and an enhancement in their local centrality and interconnectivity. Failure to reconfigure the network topology was predictive for errors, indicating that anticipatory network reconfigurations are crucial for successful task performance. On the basis of a unique network decoding approach, we also develop a general framework for the identification of characteristic patterns in complex networks, which is applicable to other fields in neuroscience that relate dynamic network properties to behavior.

graph theory | attention | cognitive control

The human brain forms a highly complex network that is organized into a large number of specialized regions. During goal-directed behavior, like the preparation of an upcoming task, relevant cortical regions are anticipatorily modulated (1–5), which has been shown to facilitate the detection and analysis of task-relevant stimuli (6–13).

However, little is known about how these task-specific adjustments are integrated across distinct brain regions and how preparatory mechanisms are reflected in a large-scale network topology (14–16). It has been shown that attention can modulate interarea correlations between distant cortical regions, independent from changes in regional blood flow (17–19). However, these studies were usually limited to a small selection of cortical regions (2, 7, 15, 18–20). With recent developments in functional connectivity analysis, it has become possible to study the role of large-scale networks for cognitive processing and to quantify network properties using global and local graph theoretical measures (21–26).

On the one hand, task preparation involves dynamic adjustments in regions that carry out computations that are specific to a given task. On the other hand, it also requires the stable maintenance of task goals (7) and reconfigurations of the network based on these goals. Given these characteristics and the organization of brain networks into modules with distinct functional properties (27, 28), we hypothesized that task-specific processes, whose involvement varies from trial to trial, are reflected in dynamic adjustments of more peripheral components of the brain network. We further hypothesized that task goals are represented in a stable network core that we expected to be densely connected and to have direct access to large portions of the network (29, 30).

According to this reasoning, reconfiguration of brain networks for different tasks should involve dynamic adaptations focused on task-relevant areas in the periphery of the brain network, but should also influence core–periphery interactions. Given the high interconnectivity of frontal areas and their role in sustaining attentional control, we further expected that frontal areas would feature prominently in the core. In contrast, we expected areas more closely related to stimulus processing to be part of the periphery.

We tested these predictions using functional magnetic resonance imaging (fMRI) in healthy adults during the preparation phase of a demanding visual discrimination task (Fig. 1A). The aim of our study was twofold. First, we aimed at examining how functional brain networks are reconfigured in the context of changing task demands. This was done by investigating whether we could predict from the network topology during task preparation for which task (i.e., color or motion; Fig. 1A) the participant was preparing. Importantly, our analyses focus on the preparation interval of the task, thus allowing us to investigate top–down-controlled network reconfigurations independent of bottom–up stimulus effects or motor execution. Second, and crucially, to test how relevant these reconfigurations are for task performance, we planned on investigating whether we could predict from the topology of preparatory network reconfiguration whether the task would be performed correctly. On the basis of functional neuroimaging studies focusing on local population activity (5, 15, 29) we expected dynamic adjustments to be centered on task-relevant visual areas V4 (involved in color processing) and hMT (motion processing).

Functional connectivity graphs (Fig. 1C) were derived from fMRI data by calculating, for each subject, the temporal correlation (coherence) between a functionally defined set of 70 brain regions (nodes) that were found to be involved in task preparation (Fig. 1B). The lack of previous studies on topological network properties during task preparation motivated the development of a completely data-driven, inverse modeling framework. Using graph theory, we extracted a comprehensive set of global and local network characteristics that were combined to create a network fingerprint for each subject and condition (schematic visualization in Fig. 2A). A pattern classification algorithm was applied to identify patterns common to task condition-specific network topologies and revealed nodes and network characteristics most informative for distinguishing the network states during preparation for different tasks (Fig. 2B; see *Materials and Methods* for details on the experimental paradigm and analysis).

Fig. 1. Paradigm and functional network construction. (*A*) A letter cue instructed participants to prepare for a task ("C" for color or "M" for motion) or was uninformative regarding the upcoming task ("N" for neutral). After a variable preparation interval of 5,000–9,000 ms a target was presented that required a color or motion judgment (*Materials and Methods*). (*B*) Searchlight analysis of BOLD activation data shows a functionally defined network that was activated for preparatory trials (cues C and M) compared with no-preparation trials (cue N), and that was used to define 70 non-overlapping nodes. (*C*) Time courses from the preparation periods (cue onset until one TR immediately before target onset; frames in boldface type in *A*) were extracted for each node and concatenated over trials to calculate pairwise correlation matrices for each subject and condition. Displayed are three randomly chosen node time courses of 400 s from one participant, the condition-specific time windows used for concatenation, and resulting task-specific networks.

Results

Network Construction. Comparing blood oxygen level dependent (BOLD) activity during preparation and no-preparation trials, we identified a widely distributed set of cortical and subcortical regions involved in top–down preparatory control (Fig. 1*B, Left* and *SI Materials and Methods*). Most importantly, this network included color-sensitive area V4 and motion-sensitive area hMT, as well as a number of frontal and parietal areas previously associated with task preparation and top–down attentional control (6, 7, 30–33). The preparatory network was used to derive 70 spherical, nonoverlapping network nodes (Fig. 1*B, Center*) from which low-frequency (0.06–0.12 Hz) BOLD time series were extracted (23). Pairwise correlations between nodes were computed and used to construct the functional network graphs for each subject and condition (Fig. 1*C*).

Network Decomposition. To divide the network into core and periphery, we used *k*-core decomposition, a recursive pruning

strategy (34) that has previously been applied to structural brain imaging data (35, 36). This approach identified a core with 24 nodes (58% in frontal cortex) and a periphery consisting of the remaining 46 nodes, including V4 and hMT (13% in frontal cortex; Fig. 3 *A* and *B*). To investigate the functional properties of the core and periphery subgraphs, we estimated their robustness to simulated failure. We applied a random edge attack (36, 37), which revealed a clear distinction between core and periphery. In contrast to the periphery, the core was highly error resilient (*P* < 0.001; 1,000 permutations), indicated by its conserved global efficiency even when large proportions of this subgraph were removed (Fig. 3*C*). When considering the effect of the simulated failure on the overall network (Fig. 3*D*), we found that the core attack, as expected by its densely connected structure, had a bigger impact on the global efficiency (*P* < 0.001; 1,000 permutations).

Network Reconfiguration. To test our prediction that task preparation involves the reconfiguration of core–periphery interactions, we included two graph measures for the quantification of these interactions. Core centrality quantifies the centrality of the core by calculating the number of shortest paths between any noncore nodes that pass through the core (36). Core closeness reflects the ease of information flow between a periphery node and the core and is defined as the inverse average distance to all core nodes. Anticipatory reconfigurations of network properties were quantitatively assessed using these measures in addition to an established set of 9 local and 10 global graph-theoretical measures (21 measures in total; *Materials and Methods* and Fig. S1) (25, 26). Our inverse modeling framework (Fig. 2*B*) combined all network measures into one high-dimensional description of a network

Fig. 2. Schematic of the inverse network modeling approach. (*A*) A network graph is characterized by multiple topological measures (here shown for degree, clustering, and centrality), each focusing on different functional aspects of the connectivity structure, resulting in a rich description (fingerprint) of the functional connectome. (*B*) A pattern classifier is trained on fingerprints of all but one subject to detect possible network reconfigurations between conditions. Normalized weights of the learned classification model are used to infer the relative importance of individual graph measures and nodes for the discrimination. The resulting model is validated using the remaining subject (leave-one-subject-out). Darker colors indicate higher values.

NEUROSCIENCE

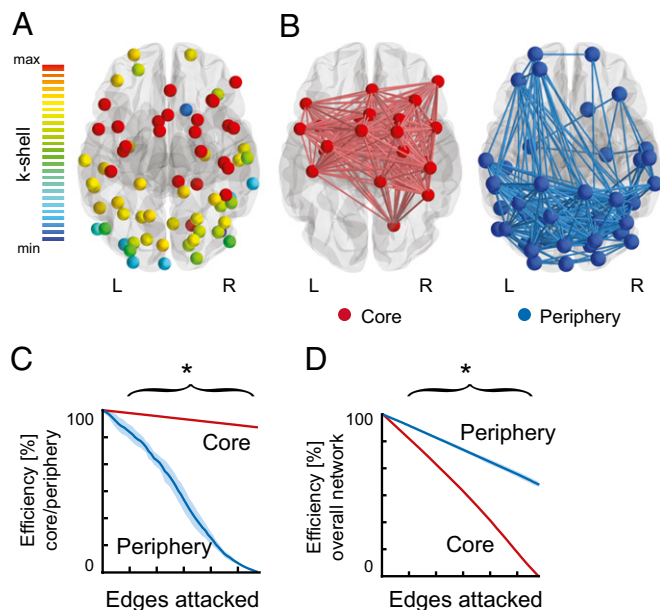PSYCHOLOGICAL AND COGNITIVE SCIENCES

Fig. 3. Network decomposition and error resilience. (*A*) *k*-core decomposition assigned each node a *k*-shell index. (*B*) *k*-shell$_{max}$ nodes form the densely connected network core (red) and the remaining nodes form the periphery (blue). (*C* and *D*) Simulated attack shows the error resistance of the core, relative to the periphery (*C*), and its importance for the efficiency of information transfer in the overall network (*D*) when increasing numbers of edges are removed. Asterisks indicate statistical significance (*$P < 0.001$; 1,000 permutations); shaded areas indicate SEM.

state (fingerprint) and used a pattern classification algorithm (sparse multinomial logistic regression with leave-one-subject-out cross-validation) to detect characteristic patterns and network nodes that were most informative for distinguishing the preparatory network states under investigation.

Results showed that we could distinguish with a high accuracy between color and motion preparation on the basis of network topologies during the task preparation interval (classification performance 94.4%, $P = 8.9 \times 10^{-5}$; 10,000 permutations). Importantly, our approach also successfully predicted whether subjects would perform the upcoming task correctly or incorrectly. Again, this prediction was based on network states of the preparation period alone (classification performance color task, 77.8%, $P = 3.1 \times 10^{-4}$; motion task, 88.9%, $P = 2.7 \times 10^{-4}$; 10,000 permutations each).

The strength of our inverse modeling approach is the data-driven selection of discriminative network nodes and corresponding measures, which revealed a highly structured reconfiguration pattern (Fig. 4 *A–C*). Confirming our hypothesis, preparation was characterized by dynamic adjustments centered on V4 and hMT bilaterally. When a perceptual area became task relevant (e.g., V4 during the color task), it showed a tighter integration into the large-scale network topology, as reflected exclusively in three local graph measures (compare classifier weights in the leftmost plot in Fig. 4*A*): clustering (reflecting interconnectivity: neighbors of a node are themselves neighbors, forming a closed triangle structure), centrality (reflecting hubness: relative amount of shortest paths crossing a node), and core closeness. In contrast, the integration of the task irrelevant visual area (e.g., hMT during the color task) was reduced (Fig. 4*B*). Modulation in core closeness, but not in closeness centrality (closeness to the whole network) shows that the change in closeness was specific to the core.

In error trials, the decreased integration of V4 and hMT was accompanied by a reduction in core centrality (Fig. 4 *A* and *C*), a global measure that can be interpreted as the topological ability

of the network core to integrate and control information flow. As no differences in mean connectivity were found (*SI Materials and Methods*), the loss in core centrality cannot be attributed to a general breakdown of information flow during error trials. Instead, it can be interpreted as maladaptive core–periphery interactions resulting in information transfer omitting the core.

Preparation and BOLD Amplitude. In comparison with the reconfigurations in network topology, we found only small or no effects for changes in mean activity. We adapted the analysis to classify the conditions under investigation on the basis of the mean BOLD amplitude in all 70 nodes. Whereas it was possible to decode with marginal significance whether subjects were preparing for the color or the motion task (classification performance, 61%; $P = 0.058$; permutation test), we were not able to predict the task performance (classification performance color task, 44%; motion task, 55%; all P values >0.2). Similar dissociations between mean response amplitude and connectivity have been previously reported in other cognitive domains (15, 17, 19). Thus, it appears unlikely that the observed topological changes can be explained by differences in BOLD amplitude.

Discussion

We demonstrate how functional networks flexibly adjust their connectivity structure to facilitate performance in an upcoming visual discrimination task. By focusing on a graph theoretical perspective, we uncover substantial topological changes in the
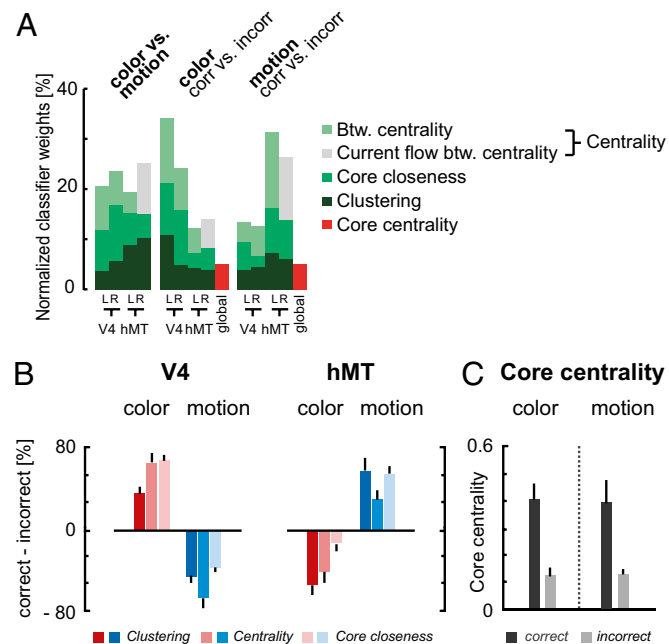

Fig. 4. Reconfiguration patterns in network topology. (*A*) Stacked bar plots show the relative importance of nodes and measures for the classification of preparatory conditions. Reconfigurations are centered on V4 and hMT, bilaterally. For the prediction of the task (color vs. motion) topological adjustments of V4 and hMT were equally predictive. For the prediction of task performance (correct vs. incorrect) reconfigurations of the respective task-relevant visual area (i.e., V4 for color, hMT for motion) became more accentuated. (*B*) Effective integration of task-relevant areas into the large-scale network topology. Color preparation during correct trials is characterized by a heightening in clustering, centrality, and core closeness in color-sensitive area V4 and a reduction of the same measures in motion-sensitive area hMT. The effect is mirrored for hMT during motion preparation. (*C*) Higher centrality of the core during correct preparation trials. Error bars indicate SEM.

network structure and capture aspects of anticipatory network reconfigurations that cannot be derived from local BOLD activation data alone. Our findings suggest that preparatory attention can selectively modulate the topological connectivity structure based on current task goals. Observed network modulations include an enhanced integration of task-relevant as well as a reduced integration of task-irrelevant regions. This observation emphasizes the flexibility of the large-scale network architecture for adapting to rapidly changing task demands. Our results show that reconfiguration of the large-scale connectivity pattern is tightly linked to behavioral performance and add to a growing body of evidence showing the importance of network reconfiguration for various cognitive functions (21, 23) including attention and working memory, which was, however, so far mostly based on neurophysiological data (2, 15, 23, 38, 39).

Network Core and Effective Integration of Task-Relevant Areas. The core is a highly connected and error-resilient network structure that is important for efficient information transfer in the network. In that sense it is closely related to the concept of densely connected "rich-club" nodes (36). Given these topological properties and its location primarily in frontal cortex, the core appears to be in an ideal position to exert control over the periphery (4, 30, 40, 41). We interpret the increased core closeness of task-relevant areas to reflect an enhancement in bidirectional information flow. The tighter integration of sensory regions with the frontal core complements previous findings focusing on altered connectivity between frontal and individual sensory regions (20) and can reflect top–down control but also anticipatory facilitation for more efficient routing of sensory information upon target presentation to higher-order cognitive areas involved in perceptual evaluation (20), decision making (42), and motor control. The fact that fewer shortest periphery-to-periphery paths crossed the core (i.e., reduced core centrality) during preparation in incorrect trials further supports our assumption that task preparation (and potentially other cognitive control mechanisms) is partly dependent on a highly connected, central network structure with inherent topological properties that enable stable representation of current task goals and efficient control of information flow.

In the network's periphery, we observed task-specific modulations in graph metrics (i.e., clustering and centrality) centered on visual areas V4 and hMT. The enhancement in local clustering is commonly believed to reflect an increase in distinct local information processing (25, 26). Here we show that the local interconnectivity can be dynamically adjusted for task-relevant and irrelevant areas, possibly allowing for more stable feature-specific processing upon target presentation, and that this adjustment is critical for successful task performance.

Centrality is based on the concept of the shortest path available to transfer information from one node to another. If many shortest paths are crossing a certain node, this node might be crucial to efficient communication (26). During visual stimulation, neural responses at any level of the visual hierarchy result from a mixing pattern of bottom–up afferents from sensory areas and top–down signals from higher areas (1, 18). It is plausible that the enhanced centrality preceding correct trials reflects an anticipatory embedding of task-relevant visual areas into a connectivity structure that facilitates the integration of visual signals upon target presentation (19).

The co-occurrence of enhanced clustering and centrality/core closeness in task-relevant visual areas reflects two contrasting but complementary properties of functional brain networks. The local interconnectivity of brain regions allows for distinct processing of sensory attributes that need to be globally integrated to achieve coherent behavioral performance (43). Importantly, anticipatory adjustments of the large-scale connectivity structure during successful task preparation revealed a dynamic interplay of both local segregation and global integration.

Methodological Considerations. The application of graph theory has proved to be a powerful tool for the analysis of complex brain networks (21, 25). However, the availability of a large set of abstract measures leads also to technical challenges. Little is known about the functional relevance or interpretation of graph measures (26), which makes it crucial to explore their relation to human behavior. Given the lack of studies exploring differences between graph measures, preselecting a subset of graph measures to focus analyses on is a questionable approach. On the other hand, including all measures and testing their relevance independently leads to the ensuing problem of multiple comparisons (14). Our inverse modeling approach tackles this problem by combining all available measures into one statistical model (fingerprint). Using pattern classification and cross-validation, important measures and their functional relevance are investigated in an unbiased fashion. We consider the data-driven selection of network characteristics as a substantial improvement that helps to increase objectivity in exploratory network analysis and might prospectively serve to define more concrete hypotheses about dynamic reconfigurations in specific network characteristics. In our study, the number of included participants is rather small. It is therefore desirable to replicate our findings with a larger sample size in the future.

Conclusion

We found the human large-scale network architecture to be dynamically adjusted during preparation for an upcoming task. Consistent with our hypotheses, we found (*i*) that task preparation changed the interaction of a densely connected, frontally dominated core with peripheral areas specific for perceptual processing in the respective task and (*ii*) that changes in network topology were centered on task-relevant visual areas. Most importantly, the observed network reconfigurations were (*iii*) consistent across participants and predictive for the success of subsequent behavior. This consistency underscores the importance of dynamic reconfigurations in large-scale brain networks for task preparation and reveals important insights into the mechanisms underlying human behavioral flexibility.

Materials and Methods

Participants. Ten healthy volunteers (5 males, mean age 25.3 y) participated with informed consent in accordance with the local ethics committee of the University Hospital in Cologne, Germany. After exclusions for incomplete scans, 9 participants were retained for subsequent analyses. All were right-handed, had normal or corrected-to-normal vision, and had no history of psychiatric or neurological diseases and no structural brain abnormalities.

Experimental Paradigm. Target stimuli consisted of 200 colored and moving dots (0.06° × 0.06° each; lifetime, 50 ms; speed, 14°/s) randomly positioned in a circular fashion around the center of the screen (covering a visual angle of 8°). The dominant movement direction was either inward or outward. We included random movement, such that only a certain percentage of all dots moved coherently inward or outward. The dominant color was either red or blue. Three distractor colors were included that had the same luminance as the target colors (green, yellow, and purple). Depending on a letter cue (C or M) presented at the beginning of each trial, participants had to prepare for either the color or the motion task. In the color condition, participants had to indicate by button press whether the dominant color was red or blue, and in the motion condition participants had to indicate whether the dominant movement direction was inward or outward. Participants were instructed to respond as fast and as correctly as possible. As a control condition, we included trials where participants were not able to prepare for the upcoming task (cue N). Targets in nonpreparation trials consisted either of stationary colored dots or of moving gray dots, so that participants unambiguously knew which task to perform upon target presentation.

Task difficulty, determined by the coherence of the task-relevant feature, was adapted individually for each participant in a 12-min practice session before the fMRI experiment. On the basis of a pilot study, color coherence values were set to 34% and motion coherence values were adjusted to obtain similar reaction times and error rates. These values were then chosen as starting values for the fMRI session during which the values were further

adapted, if necessary. The behavioral results confirmed that there were no differences in task difficulty between the tasks [reaction times, color, 705 ms ± 15 SEM; motion, 687 ms ± 16 SEM; $t_{(8)} = 1.41$; $P > 0.20$]. Also, we found no differences in error rates [color, 14.78 ± 2.29 SEM; motion, 11.44 ± 1.65 SEM; $t_{(8)} = 1.53$; $P = 0.17$].

Timing was as follows: A cue was presented for 1,000 ms, followed by a variable preparation delay of 5,000, 7,000, or 9,000 ms. The target was presented for 1,000 ms, followed by an intertrial interval of 3,000 ms. Each condition (neutral, color, motion) was presented 72 times in counterbalanced order. After 18 consecutive trials, visual feedback was given to inform about errors in the previous task block. The feedback was followed by a null event (10–14 s). The total duration of the experiment was 49 min.

Data Acquisition and Analysis. Functional data were acquired on a Siemens Trio 3T scanner, using an echo planar imaging sequence with 30 interleaved axial slices of 3 mm [field of view 192 mm, 3 × 3 mm in-plane, repetition time (TR) 2 s, echo time 30 ms, flip angle = 90°], as well as a T1-weighted high-resolution MDEFT scan. Image preprocessing was performed using the Oxford Center for Functional Magnetic Resonance Imaging of the Brain (FMRIB) Software Library (FSL). Unsmoothed functional volumes were motion and slice-time corrected (Fig. S2 for frequency of head motion).

Node Definition. Preparation and no-preparation conditions were modeled using a general linear model (GLM) and resulting parameter estimates were subjected to a multivariate searchlight analysis (radius 8 mm, across-participant cross-validation) to functionally define a map of brain regions generally involved in task preparation [i.e., (color and motion) vs. neutral; Fig. 1B]. This map was parcellated into 70 nonoverlapping nodes (radius = 12 mm). For more details, see SI Materials and Methods and Table S1.

Network Construction. For each fMRI dataset, linear and quadratic trends were removed and potential sources of global effects were regressed out (estimated movement parameters; global mean of each trial). Resulting voxel time courses were shifted by 6 s to account for the hemodynamic lag (44). For each condition the relevant time points from the preparation delay were extracted (excluding the TR immediately before target presentation) and concatenated over trials [total time points (average ± SEM): color correct, 231.3 ± 7.1; motion correct, 238.7 ± 4.7; color incorrect, 56.7 ± 7.1; motion incorrect, 49.3 ± 4.7]. Mean regional BOLD time series were then subjected to a wavelet decomposition to reconstruct wavelet coefficients in the 0.06- to 0.12-Hz range (scale two). The correlation (coherence) between all possible pairs of regions was calculated to construct four 70 × 70 weighted connectivity matrices, one for each condition. Negative correlations and those that did not pass false discovery rate (FDR) correction [FDR($q = 0.01$)] were set to zero.

Network Decomposition. Functional connectivity matrices were Fisher z transformed and averaged over all preparation conditions and subjects. In contrast to the individual data, the group-averaged matrix was thresholded to retain only 20% of the strongest connections and converted to a binary graph. K-core decomposition first removes all nodes with one connection only (including their edges) and assigns them to the $k = 1$ shell. The procedure is then repeated for all nodes with two or fewer connections, which are assigned to the $k = 2$ shell. This is repeated with increasing k, until all nodes are assigned to a k-shell (Fig. 3A). Second, on the basis of the k-shell index, nodes are divided into the core (nodes with k-shell index = k_{max}) and the periphery (nodes with indexes smaller than k_{max}). A control analysis confirmed the stability of the core when analyzing all conditions separately (Fig. S3).

Graph Analysis: Network Quantification. To characterize functional network topologies, a list of 21 weighted network measures (10 local and 11 global measures: namely, local and global degree; average shortest path length; local and global clustering; assortativity; transitivity; modularity; local, global, cost, and nodal efficiency; small-world scalar; betweenness and current flow betweenness centrality; eigenvector, closeness, and core centrality; Page-Rank; vulnerability; and core closeness) were calculated separately for each subject and condition and concatenated into a network fingerprint containing 711 entries in total (i.e., 10 local measures × 70 nodes plus 11 global measures), per subject. All metrics were calculated using the networkX software package (http://networkx.lanl.gov; corresponding formulas are listed in SI Materials and Methods and interdependence of metrics is shown in Fig. S1).

Network Decoding. For each subject and condition, indexes of the network fingerprint were transformed to z-scores and subjected to a pattern classification algorithm [sparse multinomial logistic regression (45), $\lambda = 0.1$, implemented in PyMVPA (46)]. The classifier was trained on all but one subject and the remaining subject was used as an independent test set. This leave-one-subject-out procedure was repeated until every subject had been used in the test set once. The classification performance (for decoding tasks, i.e., color vs. motion, and performance, i.e., correct vs. incorrect separately for each task) was assessed and the resulting classification weights were taken as indicators for the relative importance of each node and measure for the classification (Fig. 2). For values of the discriminative graph measures see Table S2. To determine the statistical significance of the classification performance and related weights, we performed a nonparametric permutation test with 10,000 permutations (47). All reported weights of the classification function were significant ($P < 0.05$) and were corrected for multiple comparisons (711, regions and metrics), using FDR ($q = 0.05$).

1. Kanwisher N, Wojciulik E (2000) Visual attention: Insights from brain imaging. *Nat Rev Neurosci* 1:91–100.
2. Donner TH, et al. (2007) Population activity in the human dorsal pathway predicts the accuracy of visual motion detection. *J Neurophysiol* 98:345–359.
3. Wylie GR, Javitt DC, Foxe JJ (2006) Jumping the gun: Is effective preparation contingent upon anticipatory activation in task-relevant neural circuitry? *Cereb Cortex* 16:394–404.
4. Bressler SL, Tang W, Sylvester CM, Shulman GL, Corbetta M (2008) Top-down control of human visual cortex by frontal and parietal cortex in anticipatory visual spatial attention. *J Neurosci* 28:10056–10061.
5. Langner R, et al. (2011) Modality-specific perceptual expectations selectively modulate baseline activity in auditory, somatosensory, and visual cortices. *Cereb Cortex* 21:2850–2862.
6. Sakai K, Passingham RE (2006) Prefrontal set activity predicts rule-specific neural processing during subsequent cognitive performance. *J Neurosci* 26:1211–1218.
7. Sakai K, Passingham RE (2003) Prefrontal interactions reflect future task operations. *Nat Neurosci* 6:75–81.
8. Morishima Y, et al. (2009) Task-specific signal transmission from prefrontal cortex in visual selective attention. *Nat Neurosci* 12:85–91.
9. Serences JT, Boynton GM (2007) Feature-based attentional modulations in the absence of direct visual stimulation. *Neuron* 55:301–312.
10. Cohen MR, Maunsell JHR (2009) Attention improves performance primarily by reducing interneuronal correlations. *Nat Neurosci* 12:1594–1600.
11. Mitchell JF, Sundberg KA, Reynolds JH (2009) Spatial attention decorrelates intrinsic activity fluctuations in macaque area V4. *Neuron* 63:879–888.
12. Ress D, Backus BT, Heeger DJ (2000) Activity in primary visual cortex predicts performance in a visual detection task. *Nat Neurosci* 3:940–945.
13. Pestilli F, Carrasco M, Heeger DJ, Gardner JL (2011) Attentional enhancement via selection and pooling of early sensory responses in human visual cortex. *Neuron* 72:832–846.
14. Siegel M, Donner TH, Engel AK (2012) Spectral fingerprints of large-scale neuronal interactions. *Nat Rev Neurosci* 13:121–134.
15. Hipp JF, Engel AK, Siegel M (2011) Oscillatory synchronization in large-scale cortical networks predicts perception. *Neuron* 69:387–396.
16. Gross J, et al. (2004) Modulation of long-range neural synchrony reflects temporal limitations of visual attention in humans. *Proc Natl Acad Sci USA* 101:13050–13055.
17. Haynes JD, Tregellas J, Rees G (2005) Attentional integration between anatomically distinct stimulus representations in early visual cortex. *Proc Natl Acad Sci USA* 102:14925–14930.
18. Friston KJ, Büchel C (2000) Attentional modulation of effective connectivity from V2 to V5/MT in humans. *Proc Natl Acad Sci USA* 97:7591–7596.
19. Freeman J, Donner TH, Heeger DJ (2011) Inter-area correlations in the ventral visual pathway reflect feature integration. *J Vis* 11:11.
20. Zanto TP, Rubens MT, Thangavel A, Gazzaley A (2011) Causal role of the prefrontal cortex in top-down modulation of visual processing and working memory. *Nat Neurosci* 14:656–661.
21. Bressler SL, Menon V (2010) Large-scale brain networks in cognition: Emerging methods and principles. *Trends Cogn Sci* 14:277–290.
22. Bassett DS, Meyer-Lindenberg A, Achard S, Duke T, Bullmore E (2006) Adaptive reconfiguration of fractal small-world human brain functional networks. *Proc Natl Acad Sci USA* 103:19518–19523.

23. Bassett DS, et al. (2011) Dynamic reconfiguration of human brain networks during learning. *Proc Natl Acad Sci USA* 108:7641–7646.
24. Kitzbichler MG, Henson RNA, Smith ML, Nathan PJ, Bullmore ET (2011) Cognitive effort drives workspace configuration of human brain functional networks. *J Neurosci* 31:8259–8270.
25. Bullmore E, Sporns O (2009) Complex brain networks: Graph theoretical analysis of structural and functional systems. *Nat Rev Neurosci* 10:186–198.
26. Rubinov M, Sporns O (2010) Complex network measures of brain connectivity: Uses and interpretations. *Neuroimage* 52:1059–1069.
27. Meunier D, Lambiotte R, Bullmore ET (2010) Modular and hierarchically modular organization of brain networks. *Front Neurosci* 4:200.
28. Power JD, et al. (2011) Functional network organization of the human brain. *Neuron* 72:665–678.
29. Tootell RB, et al. (1995) Functional analysis of human MT and related visual cortical areas using magnetic resonance imaging. *J Neurosci* 15:3215–3230.
30. Corbetta M, Shulman GL (2002) Control of goal-directed and stimulus-driven attention in the brain. *Nat Rev Neurosci* 3:201–215.
31. Maunsell JH, Treue S (2006) Feature-based attention in visual cortex. *Trends Neurosci* 29:317–322.
32. Brass M, von Cramon DY (2002) The role of the frontal cortex in task preparation. *Cereb Cortex* 12:908–914.
33. Brass M, von Cramon DY (2004) Decomposing components of task preparation with functional magnetic resonance imaging. *J Cogn Neurosci* 16:609–620.
34. Carmi S, Havlin S, Kirkpatrick S, Shavitt Y, Shir E (2007) A model of Internet topology using k-shell decomposition. *Proc Natl Acad Sci USA* 104:11150–11154.
35. Hagmann P, et al. (2008) Mapping the structural core of human cerebral cortex. *PLoS Biol* 6:e159.
36. van den Heuvel MP, Sporns O (2011) Rich-club organization of the human connectome. *J Neurosci* 31:15775–15786.
37. Achard S, Salvador R, Whitcher B, Suckling J, Bullmore E (2006) A resilient, low-frequency, small-world human brain functional network with highly connected association cortical hubs. *J Neurosci* 26:63–72.
38. Gregoriou GG, Gotts SJ, Zhou H, Desimone R (2009) High-frequency, long-range coupling between prefrontal and visual cortex during attention. *Science* 324:1207–1210.
39. Palva JM, Monto S, Kulashekhar S, Palva S (2010) Neuronal synchrony reveals working memory networks and predicts individual memory capacity. *Proc Natl Acad Sci USA* 107:7580–7585.
40. Armstrong KM, Fitzgerald JK, Moore T (2006) Changes in visual receptive fields with microstimulation of frontal cortex. *Neuron* 50:791–798.
41. Ruff CC, et al. (2006) Concurrent TMS-fMRI and psychophysics reveal frontal influences on human retinotopic visual cortex. *Curr Biol* 16:1479–1488.
42. Philiastides MG, Auksztulewicz R, Heekeren HR, Blankenburg F (2011) Causal role of dorsolateral prefrontal cortex in human perceptual decision making. *Curr Biol* 21:980–983.
43. Tononi G, Sporns O, Edelman GM (1994) A measure for brain complexity: Relating functional segregation and integration in the nervous system. *Proc Natl Acad Sci USA* 91:5033–5037.
44. Aguirre GK, Zarahn E, D'Esposito M (1998) The variability of human, BOLD hemodynamic responses. *Neuroimage* 8:360–369.
45. Krishnapuram B, Carin L, Figueiredo MA, Hartemink AJ (2005) Sparse multinomial logistic regression: Fast algorithms and generalization bounds. *IEEE Trans Pattern Anal Mach Intell* 27:957–968.
46. Hanke M, et al. (2009) PyMVPA: A python toolbox for multivariate pattern analysis of fMRI data. *Neuroinformatics* 7:37–53.
47. Nichols TE, Holmes AP (2002) Nonparametric permutation tests for functional neuroimaging: A primer with examples. *Hum Brain Mapp* 15:1–25.

NEUROSCIENCE

PSYCHOLOGICAL AND COGNITIVE SCIENCES